RSC Advances

ROYAL SOCIETY OF CHEMISTRY

www.rsc.org/advances

$Cu@SiO_2$ Nanowires: Synthesis, Cathodoluminescence and SERS Response

Chunlei Pang[1], *Hao Cui*[1,2†] *& Chengxin Wang*[1,2*]

[1]*State key laboratory of optoelectronic materials and technologies, School of Physics Science and Engineering, Sun Yat-sen (Zhongshan) University, Guangzhou 510275, People's Republic of China*

[2]*The Key Laboratory of Low-carbon Chemistry & Energy Conservation of Guangdong Province, Sun Yat-sen (Zhongshan) University, Guangzhou 510275, People's Republic of China*

†These authors contributed equally to this work.* Correspondence and requests for materials should be addressed to C. X. Wang. Tel & Fax: +86-20-8411-3901, E-mail: wchengx@mail.sysu.edu.cn

Abstract:

Various shapes of Cu@SiO_2 nanowires were fabricated on Cu substrate via simple thermal evaporation of SiO within a high-frequency induction furnace. The morphology and structure of the Cu@SiO_2 nanowires were characterized by using SEM, TEM, EDS and EDX elemental mapping. The morphology and density of nanowires are controllable by adjusting the substrate temperature. The Cu cores are chemical stability at the protection of SiO_2 shell. The surface-enhanced Raman scattering (SERS) experiment of the shell-isolated nanowires showed excellent detecting performance compared with bare Cu substrate. The Cathodoluminescence (CL) investigation reveals that red, green and blue light emissions were observed in the Silica sheath simultaneously. The as-synthesized samples have potential application in long acting and ultrasensitive SERS substrate and white light sources.

Keywords: Cu nanowires; SiO_2 shell; SERS detecting; Cathodoluminescence;

Introduction:

In recent years, nanostructured materials with novel physical properties have become a focus of intense research due to their significant potential application in optoelectronic technology[1-3]. Various nanomaterials have been fabricated by different methods[4]. Among the various nanostructures, metal nanowires have attracted much attention due to their potential use as interconnects in future nanoelectronics and application possibilities[5-7]. In order to manufacture optoelectronic devices, interfaces accommodated with functional variation have been made[4, 8-11]. And a simple method for synthesis nanostructures is essential. Surface-enhanced Raman scattering (SERS) is a powerful spectroscopy technique that can provide non-destructive and ultrasensitive characterization down to single molecular level, comparable to single-molecule fluorescence spectroscopy[12, 13]. However, generally substrates based on metals such as Ag and Au, either with roughened surfaces or in the form of nanoparticles, are required to realize a substantial SERS effect, which severely limited the breadth of practical applications of SERS. Recently, Luis et al.[7] reported that the optical of Au and Ag nanoparticle systems can be tuned over a wide spectral range through SiO_2 coating that allow one to tailor surface Plasmon resonance frequencies. Dong et al.[14, 15] reported that MoO_3 sumiconducutors have also been used for local and Remote SERS. Tian et al.[12] reported an approach, which named shell-isolated nanoparticle-enhanced Raman spectroscopy, in which the Raman signal amplification is provided by gold nanoparticles with an ultrathin SiO_2 or Al_2O_3 shell. Compared with Ag, Cu is 1000 times more abundant and 100 times less expensive[6]. Developing Cu-based nanostructures has therefore emerged as a highly promising approach leading toward low-cost SERS substrate.

Here, we report the synthesis of Cu@SiO_2 nanowires on Cu substrate by simple thermal evaporation of SiO within a high-frequency induction furnace. The morphology and density of nanowires are controllable by adjusting the substrate temperature. The core-shell nanowires expressed obvious SERS active compared with

bare Cu substrate. The SiO_2 sheath can prevent oxidation of the metal inside and is believed to promote the SERS performance.[7, 12] In addition, the Cathodoluminescence (CL) investigation reveals that red, green and blue light emissions were observed in the SiO_2 sheath simultaneously.

Experimental:

The synthesis of Cu@SiO_2 nanowires was performed in a vertical high-frequency induction furnace consisting of a fused-quartz tube surrounded by the radio-frequency (RF) coil, an induction-heated cylinder made of high-purity graphite coated with a carbon fiber thermoinsulating layer and a graphite crucible which was mounted inside, as described previously[16, 17]. The carrier gas was blown into the furnace through the gas path under the graphite crucible and gone through the cavity of the graphite cylinder and then pumped out through the hole above it. SiO powder and Cu sheet were used as the solid reaction resources while Ar was employed as the carrier gas. SiO powder was loaded in the graphite tube and the copper sheets were put onto the top of graphite cylinder. Before heating, the furnace was evacuated by a mechanical pump, and then a constant gas flow of high-purity Ar was introduced, serving as carrier gas at a flow rate of 150 sccm (standard cubic centimeter per minute). The pressure was maintained at 8 KPa throughout the whole experimental process. The graphite crucible was then heated to about 1500 °C and kept for 1 h. The SiO powder evaporated from the graphite tube when heating began and the Cu@SiO_2 nanowires were synthesized on the Cu sheets where the temperature was about 1000 °C.

The morphology was investigated by field emission scanning electron microscope (FESEM, FEI Quanta 400F). The micro-structure analysis was further employed using high resolution transmission electron microscope (HRTEM, FEI Tecnai G2 F30 operated at 300 kV accelerating voltage at room temperature) attached with selected area electron diffraction (SAED) and X-ray energy dispersive spectrometer (EDS).

CL spectrum from individual nanostructure was collected by using a scanning

electron microscope (AURIGA-4523) with a field emission electron gun equipped with a CL system. The pressure in the specimen chamber was 3×10^{-4} Pa. The CL SEM-image and spectrum was collected at room temperature under the same conditions. Raman analysis and SERS test was carried out on Laser Micro-Raman Spectrometer (Renishaw inVia) analysis platform. As a widely used efficient bio-indicator, rhodamine 6G (R6G) in ethanol solution was used as probe molecules for SERS measurements. Prior to the measurements, 150 μl of 10^{-4} M R6G solution in ethanol were dropped on the nanostructured substrate with the size of 1 cm×1 cm (which correspond to 1.5×10^{-8} M/cm^2) and then air-dried. SERS and Raman spectra were acquired by a 633nm laser source at power of 0.25 mW. The integration time is 30 s and the accumulation is twice.

Results and discussion:

Figure 1 shows the SEM and TEM images of the Cu@SiO_2 nanowires. A low-magnification top view FESEM image of the sample morphology on the Cu substrate is displayed in Figure 1a. Figure 1b shows the high-magnification SEM image of the Cu@SiO_2 nanowires. It reveals that high density aligned nanowires are grown on the surface of the Cu substrate, and a catalyst particle can be obviously observed at the tip of each nanowire, which suggesting that the nanowires grew via a well-known vapor-liquid-solid (VLS) mechanism. The products with bright contrast should correspond to the metal Cu. Average diameter of the Cu@SiO_2 nanowires was 70±10nm and with length extending up to 10 μm.

The nanowires were dispersed on TEM grids for further structure analyses. Figure 1c shows the typical TEM image of a Cu@SiO_2 nanowire, the spherical catalyst particle attached to the tip of the nanowire has a diameter of about 300nm. It reveals that the nanowires seen in the SEM images are core-shell nanocables with a core of about 80±10nm and a shell of about 20±10nm. The HRTEM image of the nanowires is shown in Figure 1d, which confirms that the nanowire consist of a crystalline core surrounded by an amorphous sheath. The image shows a group of lattice planes in the crystalline core, which corresponds to {111} with interplanar

spacing of 0.2nm. The top inset is part of an electron diffraction pattern taken from the core of the nanowire. The diffraction spots in the SAED pattern of the core correspond to single-crystalline cubic Cu. The composition of the Cu@SiO_2 nanowires were analyzed using EDS attached to the TEM and EDX elemental mapping as shown in Figure 2. Figures 2b and 2c show, respectively, the EDS spectra obtained from the core and sheath by a finely focused electron probe. From these spectra, we can see that the copper concentrates mainly at the center of the nanowires, and the surrounding areas are of silicon oxide, and the composition of silicon oxide was calculated to be SiO_2. The EDS maps present the composition and distribution of the elements which confirmed the core-shell structure. Figures 2e-g show the EDX mapping of the Oxygen, Silicon, and Copper elements, respectively, which indicating that the inner core is Cu nanowire while the outer shell is SiO_2. On the basis of the above results and reports, we conclude that the as-prepared sample is core-shell Cu@SiO_2 nanowires.

In addition, we also synthesized several other kinds of Cu@SiO_2 related morphology and found that substrate temperature is the critical factor for controlling the morphology of Cu@SiO_2 nanowires. Figure 3 show four kinds of Cu@SiO_2 related morphology synthesized form relatively high temperature zone to relatively low temperature zone on the Cu substrates, which reveal the structure evolution of Cu@SiO_2 nanowires with temperature change. As seen in figure 3a and 3b, in the relatively higher temperature zone, the nanowires growth with high density on the Cu substrate, the nanowires have quite uniform diameter of less than 100 nm while the lengths of the nanowires are up to tens of micrometers. As the growth temperature decreased, the diameter increased remarkably to 130±10nm as shown in Figure 3c and 3d. The nanowires possess a core-shell structure consisting of a solid core encapsulated inside a hollow tube. Hollow cells are observed inside the nanostructures as marked by red arrows. The length of the nanowires is shorter than that in Figure 3a and 3b. When the temperature goes lower, the products are mainly dominated by pin-and octopus-like structures. As seen in Figure 3e and 3f, each octopus–like structure has a big Cu particle at its tip and more than one arm sprout from its tip.

These structures are very common for Si nanowires prepared via thermal evaporation based VLS and oxygen-assistance and other growth mechanisms[9, 10]. The typical diameters of the tips are in the range of 300-500nm. The arms are also core-shell structures and surfaces of the shell and core are smooth. Cu is filled inside part of the arms and partially filled inside other arms. In Figure 3g and 3h, the samples evolve into string of candied haws shape in which the surfaces of Cu core are not so smooth compared with other shapes. The heterogeneous diameters of the nanorods are periodic distributed. The results show that the Cu@SiO_2 nanowires were catalyzed by Cu particles via a VLS mechanism. The substrate temperature is the critical factor for controlling the diameter of the nanowires and the formation of the various kinds of Cu@SiO_2 related morphology. At high temperature, molten Cu metallic particles are formed on Cu substrate[18]. During the growth, SiO_2 precursors were continuously formed on the surface of catalyst particles. When the concentration of SiO_2 on the surface achieved a certain amount, the SiO_2 clusters will slip to the lower hemisphere of the catalyst to form nanotubes due to the low solubility of SiO_2 in the catalyst[16, 19]. The molten Cu were sucked into the nanotube due to capillary action[8, 20]. The Cu in the nanotube can act as the catalysts which lead to the formation of branched nanocables. During the cooling process, the molten Cu in the nanotubes became solid nanowires and hollow cells formed inside the core-shell structures[21]. In high temperature zone, the growth rate is higher than that in lower temperature and the diameter is smaller. In lower temperature zone, the nanowires nucleate at different position of Cu catalyst particles, which result in the formation of octopus-like structure nanowires.

As R6G has been well-characterized by SERS and resonance Raman spectroscopy[22], we use R6G as the target molecule to evaluate the performance of the Cu@SiO_2 nanowires as SERS substrate in this study. We compared the Raman spectra of R6G (1.5×10^{-8} M/cm^2) absorbed on the Cu@SiO_2 nanowires (Figure 1) and bare Cu substrate. As shown in Figure 4, Raman signals are detected very sharply from the Cu@SiO_2 nanowires, while the signals are hardly observed on the bare substrate. The main Raman active modes of the R6G were obtained indicating that the Raman signal

for R6G on the Cu@SiO_2 nanowires was significantly enhanced[23]. In particular, it was observed that the bands at 1645, 1508, 1361，1311 and 1181 cm^{-1} are corresponding to C-C stretching in the xanthene plane, C-O-C stretching, and C-H in-plane bending of the aromatic ring of R6G molecule[24, 25], respectively, while the peak at 770 cm^{-1} was due to the out-of-plane bending motion of the hydrogen atoms of the xanthenes skeleton[26]. Raman band from Cu@SiO_2 nanowires is more than 13 times stronger than that from bare Cu substrate. The SiO_2 shell around Cu nanostructure can protect the SERS-active nanostructure from contact with what is being probed. Furthermore, the Cu nanowires have good chemical stability for the SiO_2 shell can prevent oxidation of the Cu inside, which indicates that the Cu@SiO_2 nanowires array could be used as effective SERS substrate for long acting detecting.

Cathodoluminescence (CL) is an optoelectrical phenomenon whereby beam of electrons is generated by an electron gun and interacts with a luminescencent material, such as phosphor, causing the material to emit light[27]. As compared to other techniques, CL is a useful technique for the characterization of the optical properties of nanostructures because of is high spatial resolution and structural information obtained by using secondary electron (SE) imaging[27]. Low-energy cathodoluminescence was used to investigate the optical properties of the Cu@SiO_2 nanowires. The experiment was performed under vacuum conditions (~ 3×10^{-4} Pa) in order to avoid the surface chemical adsorption. Figure 5 shows a typical spectrum obtained from the Cu@SiO_2 nanowire structure at room temperature. The inset of Figure 5 shows its corresponding CL image, while its corresponding SEM image is shown in Figure 3h. It can be seen that the contrast form the nanostructure (with Cu core and SiO_2 shell) displays clear bright and light variations. This fact suggests that CL observed within the nanowire originates from the SiO_2 shell regions rather than from the Cu cores. The CL spectrum consists of one intense blue light-emission peak at ~460 nm (2.70 eV), a weak green emission at 565 nm (2.19 eV) and a red emission at about 645 nm (1.92 eV). The luminescence of various silica glasses and nanostructures has been studied extensively in recent decades[16, 27-31]. Several luminescence bands with different peaks ranging from 1.6~4.65 eV have been

obtained from both experimental measurements and theoretical calculations[28, 30]. The luminescence characteristic depends strongly on the silica structure, which is affected by the synthetic variables[27]. The emissions in Figure 5 are comparable to the previously reported for crystalline SiO_2 and amporphous SiO_2. Here, we believe that the 460 nm blue emission can be ascribed to Oxygen-deficient centres (ODCs) (such as neutral oxygen vacancies, ≡Si–Si≡, and twofold coordinated silicon defects, ≡Si–O–Si–O–Si≡) and self-trapped excitons[31]. The emission at 565 nm may be originated from the radiative recombination of the self trapped exciton[30]. The red band at 645 nm has been ascribed to nonbridging oxygen hole centres (NBOHCs, ≡Si–O•)[32, 33]. The resulting three-color emission indicates that the Cu@SiO_2 nanostructures have potential for application to white light sources.

Conclusions:

In summary, various shapes of Cu@SiO_2 nanowires have been fabricated on Cu substrate via simple thermal evaporation of SiO within a high-frequency induction furnace, which is an effective approach to synthesis metal or semiconductor filled silica systems. Cu nanowires were filled in SiO_2 nanotubes. The core-shell nanowires expressed obvious SERS active compared with bare Cu substrate. The Cu core provides Raman signal enhancement; the silica shell prevents the core from coming into direct contact with probe/analyte molecules or the surface over which these nanowires are spread[34]. Furthermore, the SiO_2 sheath can prevent oxidation of the metal inside which indicate that the Cu@SiO_2 nanowires array may have potential applications in long-acting SERS detection. The CL investigation reveals that red, green and blue light emissions were observed in the Silica sheath simultaneously. This result may inspire great interest in exploring SiO_2 nanostructures and their application in white light sources.

Acknowledgements

This work was financially supported by the National Nature Science Foundation of China (51125008, 11274392) supported this work.

Referances:

1. S. Iijima, *Nature*, 1991, **354**, 56-58.
2. A. M. M. a. C. M. Lieber, *Science*, 1998, **279**, 208-211.
3. C. Lok, *Nature*, 2010, **467**, 18-21.
4. Y. N. Xia, P. D. Yang, Y. G. Sun, Y. Y. Wu, B. Mayers, B. Gates, Y. D. Yin, F. Kim and Y. Q. Yan, *Advanced Materials*, 2003, **15**, 353-389.
5. H. Choi and S.-H. Park, *Journal of the American Chemical Society*, 2004, **126**, 6248-6249.
6. D. Zhang, R. Wang, M. Wen, D. Weng, X. Cui, J. Sun, H. Li and Y. Lu, *Journal of the American Chemical Society*, 2012, **134**, 14283-14286.
7. L. M. Liz-Marzán, *Langmuir*, 2006, **22**, 32-41.
8. Y. B. Li, Y. Bando and D. Golberg, *Advanced Materials*, 2004, **16**, 37.
9. Z. W. Pan, S. Dai, D. B. Beach and D. H. Lowndes, *Nano Letters*, 2003, **3**, 1279-1284.
10. A. Z. Jin, Y. G. Wang and Z. Zhang, *Journal of Crystal Growth*, 2003, **252**, 167-173.
11. Y. G. Wang, A. Z. Jin and Z. Zhang, *Applied Physics Letters*, 2002, **81**, 4425.
12. J. F. Li, Y. F. Huang, Y. Ding, Z. L. Yang, S. B. Li, X. S. Zhou, F. R. Fan, W. Zhang, Z. Y. Zhou and D. Y. Wu, *Nature*, 2010, **464**, 392-395.
13. S. Nie and S. R. Emory, *science*, 1997, **275**, 1102-1106.
14. B. Dong, Y. Huang, N. Yu, Y. Fang, B. Cao, Y. Li, H. Xu and M. Sun, *Chemistry – An Asian Journal*, 2010, **5**, 1824-1829.
15. B. Dong, W. Zhang, Z. P. Li and M. T. Sun, *Plasmonics*, 2011, **6**, 189-193.
16. C. L. Pang, H. Cui and C. X. Wang, *Crystengcomm*, 2011, **13**, 4082-4085.
17. C. L. Pang, H. Cui, G. W. Yang and C. X. Wang, *Nano Letters*, 2013, **13**, 4708-4714.
18. Y. Chen, Q. Zhou, X. Zhang, Y. Su, C. Jia, Q. Li, W. Kong and M. Wei, *Journal of Nanoscience and Nanotechnology*, 2010, **10**, 8375-8379.
19. I. Aharonovich, Y. Lifshitz and S. Tamir, *Applied Physics Letters*, 2007, **90**.
20. P. M. Ajayan and S. LIJIMA, *Nature*, 1993, **361**, 333-334.
21. Y. Zhong, Y. Zhang, M. Cai, M. P. Balogh, R. Li and X. Sun, *Applied Surface Science*, 2013, **270**, 722-727.
22. X. Sun, L. Lin, Z. Li, Z. Zhang and J. Feng, *Materials Letters*, 2009, **63**, 2306-2308.

23. B. Daglar, T. Khudiyev, G. B. Demirel, F. Buyukserin and M. Bayindir, *Journal of Materials Chemistry C*, 2013, **1**, 7842-7848.

24. N. Anton, P. Saulnier, A. Béduneau and J.-P. Benoit, *The Journal of Physical Chemistry B*, 2007, **111**, 3651-3657.

25. T. Gao, Y. Wang, K. Wang, X. Zhang, J. Dui, G. Li, S. Lou and S. Zhou, *ACS applied materials & interfaces*, 2013, **5**, 7308-7314.

26. H. Cui, P. Liu and G. W. Yang, *Applied Physics Letters*, 2006, **89**, 153124.

27. J. Q. Xu, H. Onodera, T. Sekiguchi, D. Golberg, Y. Bando and T. Mori, *Materials Characterization*, 2012, **73**, 81-88.

28. T. Y. Zhai, Z. J. Gu, Y. Dong, H. Z. Zhong, Y. Ma, H. B. Fu, Y. F. Li and J. N. Yao, *Journal of Physical Chemistry C*, 2007, **111**, 11604-11611.

29. J. Hu, Y. Bando, J. Zhan, X. Yuan, T. Sekiguchi and D. Golberg, *Advanced Materials*, 2005, **17**, 971-975.

30. M. A. Stevens-Kalceff, *Mineralogy and Petrology*, 2013, **107**, 455-469.

31. N. G. Shang, U. Vetter, I. Gerhards, H. Hofsäss, C. Ronning and M. Seibt, *Nanotechnology*, 2006, **17**, 3215-3218.

32. E. P. O'Reilly and J. Robertson, *Physical Review B*, 1983, **27**, 3780.

33. H. Nishikawa, R. Nakamura, R. Tohmon, Y. Ohki, Y. Sakurai, K. Nagasawa and Y. Hama, *Physical Review B*, 1990, **41**, 7828.

34. J. R. Anema, J. F. Li, Z. L. Yang, B. Ren and Z. Q. Tian, in *Annual Review of Analytical Chemistry, Vol 4*, eds. R. G. Cooks and E. S. Yeung, 2011, vol. 4, pp. 129-150.

Figure 1 (a) Top view SEM image and (b) side view image of the Cu@SiO_2 nanowires on Cu substrate. (c) TEM bright field image showing the microstructure of the nanowires, the nanowire consists of the core and outer shell. A spherical catalyst particle is attached to the tip of the nanowire with a diameter of about 300nm. (d) HRTEM image of the nanowires. The top inset is part of an electron diffraction pattern taken from Cu core of the nanowire.

Figure 2 Elemental analysis of the Cu@SiO_2 nanowire. (a) TEM image of the nanowire dispersed on a lacey carbon TEM grid. (b) and (c) are EDS spectra obtained from the core and shell marked in (a). (d-g) show the elemental mapping of Oxygen, Silicon, and Copper elementals.

Figure 3 Low-magnification (a, c, e, g) and higher-magnification (b, d, f, h) SEM images of various shapes of Cu@SiO_2 nanowires located from high temperature to relative low temperature zone on the Cu substrates, which reveal the structure evolution of Cu@SiO_2 nanowires with temperature change.

Figure 4 SERS spectrum of the R6G (1.5×10^{-8} M/cm^2) generated by the Cu@SiO_2 nanaowires substrate and the not enhanced Raman spectrum of bare Cu substrate.

Figure 5 CL spectrum of a single Cu@SiO_2 nanostructure. The inset is SEM-CL image of the corresponding Cu@SiO_2 nanostructure。

Figure 1

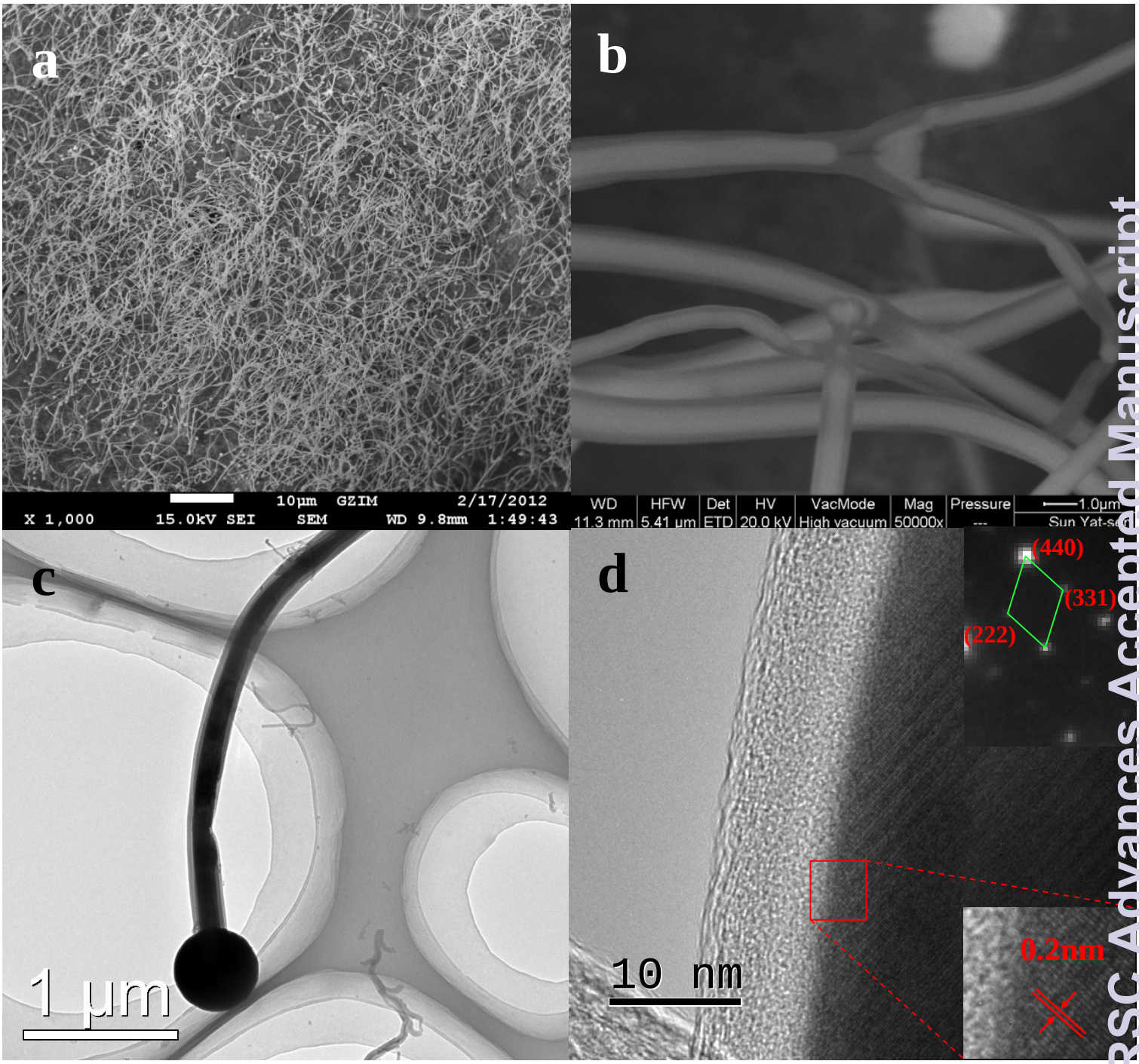

Figure 2

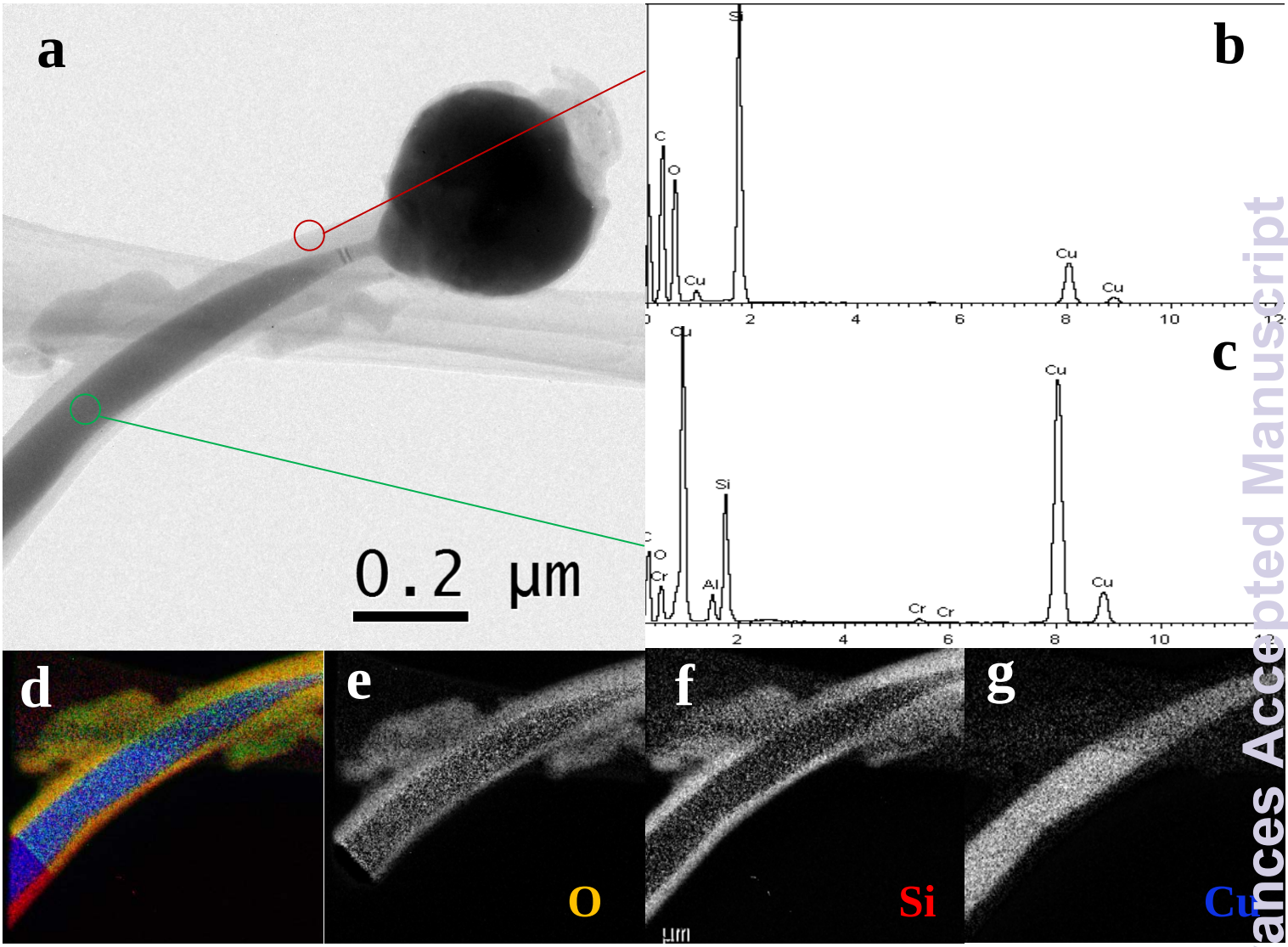

Figure 3

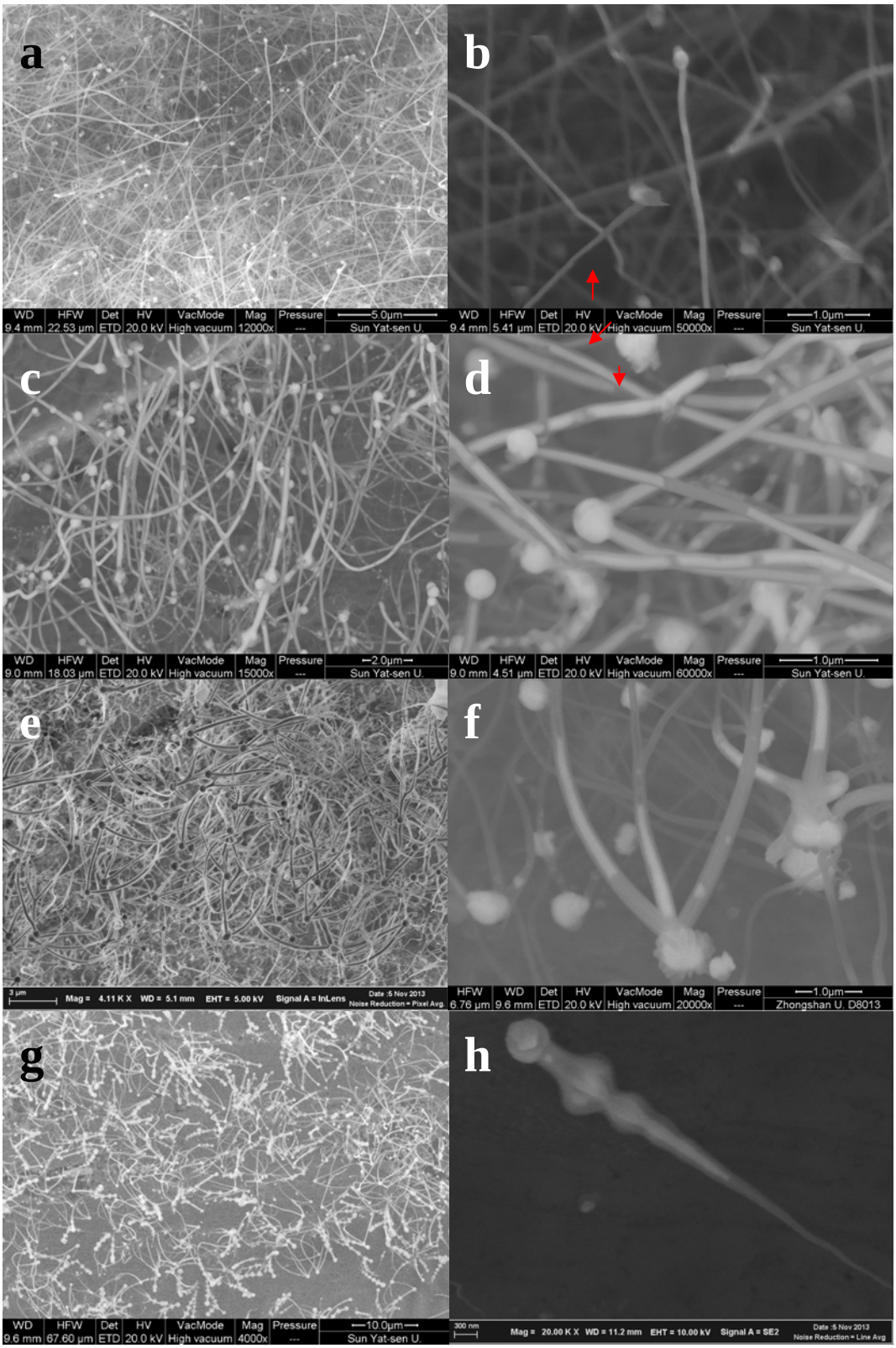

Figure 4

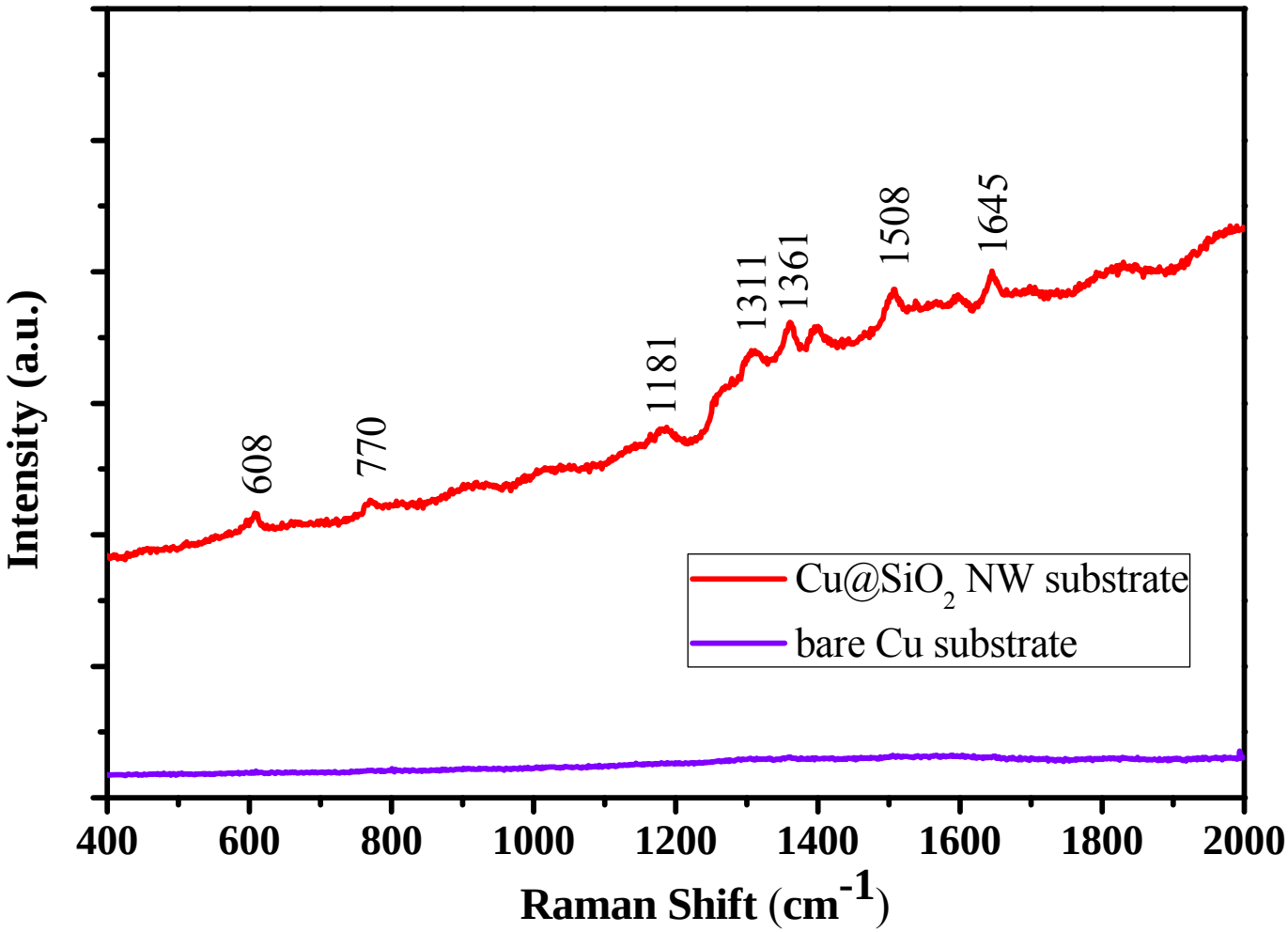

Figure 5